Supplemental Information:
Long-Distance Axonal Growth from Human Induced Pluripotent Stem Cells After Spinal Cord Injury

Paul Lu, Grace Woodruff , Yaozhi Wang, Lori Graham, Matt Hunt, Di Wu, Eileen Boehle, Ruhel Ahmad, Gunnar Poplawski, John Brock, Lawrence S. B. Goldstein and Mark H. Tuszynski

SUPPLEMENTAL FIGURES

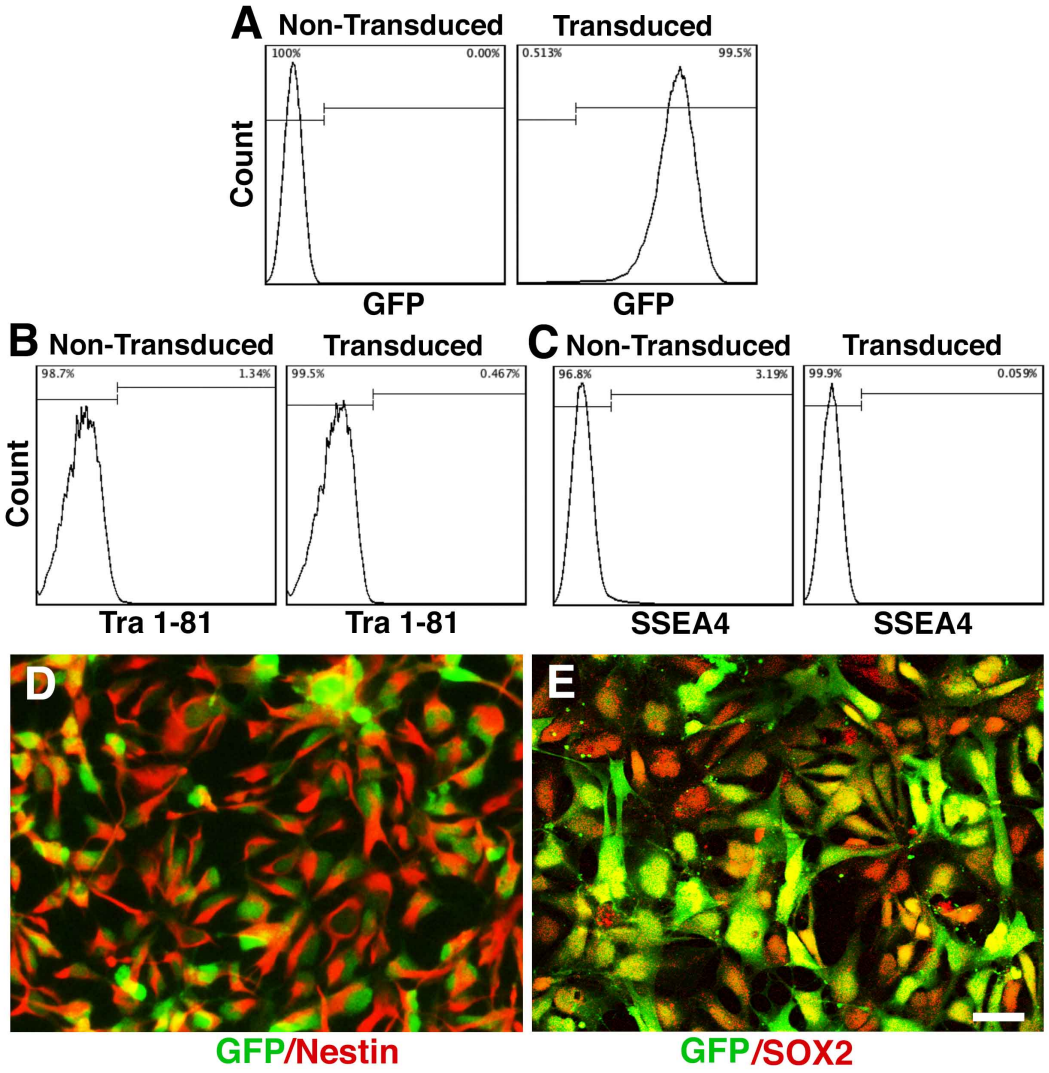

Suppl. Fig. 1 (Related to Main Fig. 1): Characterization of GFP Transduced NSCs In Vitro

(A) Analysis of GFP expression in non-transduced and lentiviral-transduced NSCs. Transduced NSCs are over 99% GFP+. **(B)** Analysis of Tra-1-81 expression in non-transduced and GFP-transduced NSCs. **(C)** Analysis of SSEA4 expression in non-transduced and GFP-transduced NSCs. **(D-E)** **GFP** (green) transduced NSCs express **Nestin** (red) and **SOX2** (red). Scale bar 28 μm.

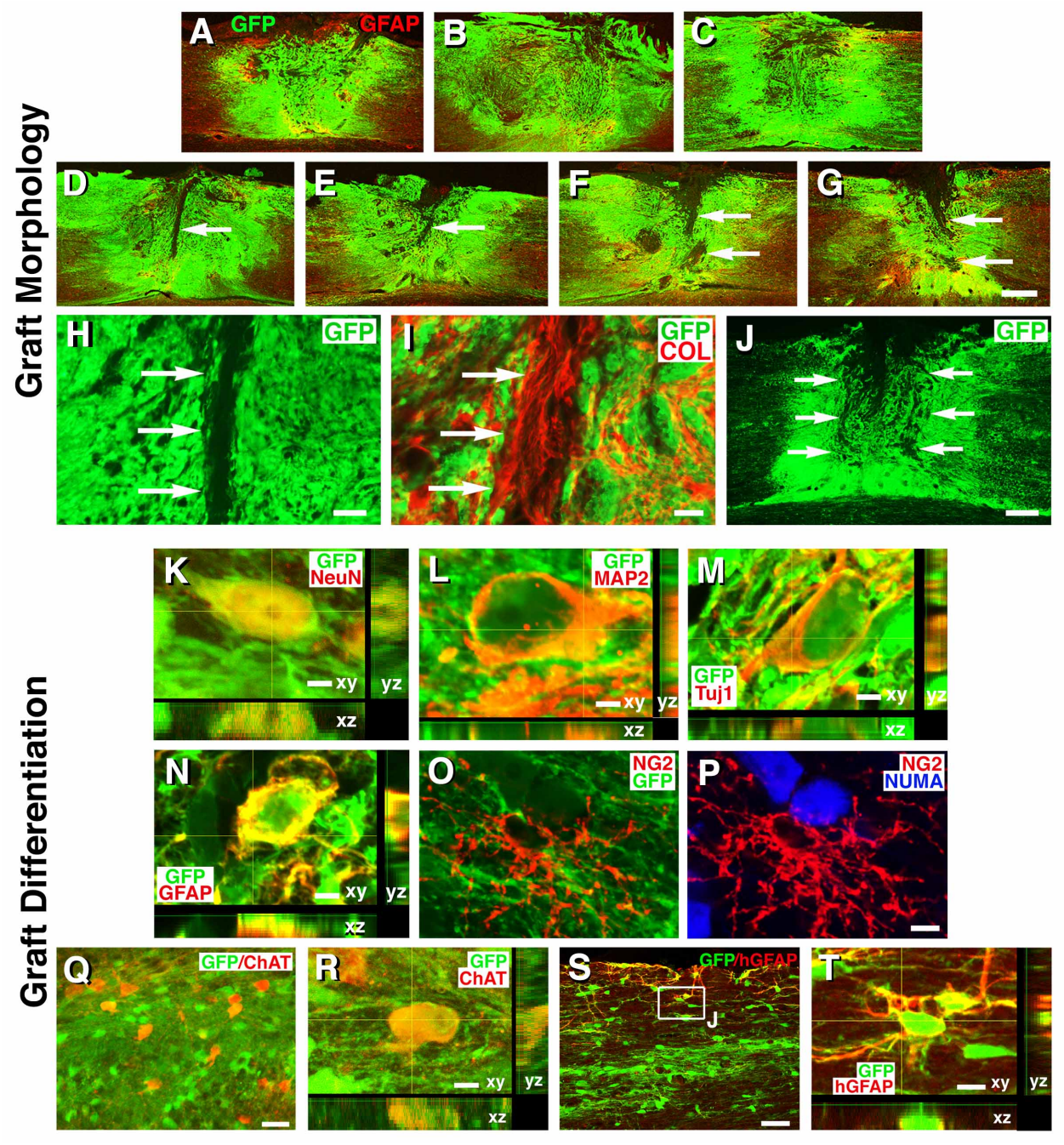

Suppl. Fig. 2 (Related to Main Fig. 1): Graft Morphology, Rift Formation, and Neural Cell Differentiation

(A-G) **GFP** and **GFAP** labeling in seven grafted subjects. Cells were present and distributed throughout each lesion cavity. However, subjects 1-3 exhibited attenuation of cell density near the central region of the graft, which would appear to limit the ability of rostral-to-caudal axonal relays to form. Grafts in subjects 4-7 exhibited a rift near the center of the graft that segregates the graft into rostral and caudal components. Horizontal sections, rostral is to the left. **(H-I)** Higher magnification view of the rift in subject 4, which separates rostral and caudal halves of graft; GFP labeled axons do not cross this gap. (**I**) The rift consisted of collagen (**COL**), most likely derived from leptomeningeal cells that migrate into the lesion site. The presence of rifts in grafts

would lead to an incomplete bridge in the lesion site, and likely block relay formation through the graft. (**J**) Higher magnification view of graft cell density attenuation in the graft core (arrows) that likely reduced the ability of implanted cells to form neural relays across the lesion site (Lu et al., 2012b).). (**K**) Confocal 5µm-thick Z-stack shows co-localization of **GFP** (grafted iPSC-NSCs) with the mature neuronal marker **NeuN**, indicating neuronal differentiation of grafted cells after 3 months in vivo. **(L-M)** GFP-labeled NSCs also co-localize with the neuronal markers **(L) MAP2** and **(M)** ßIII tubulin **(Tuj1).** (**N**) Some **GFP** labeled graft cells co-express the glial marker **GFAP,** indicating glial differentiation. (**O-P**) Human cell graft contains NG2+ oligodendrocyte progenitors that do not co-localize with either GFP or the human specific nuclear marker NUMA, suggesting that oligodendrocyte progenitors present in the graft are derived from the host. (**Q-R**) Approximately 4% of **GFP**-labeled cells in the graft express the motor neuronal marker **ChAT**. **(S-T)** Some GFP-expressing cells migrate into host spinal cord adjacent to the graft; many of these cells express the astrocyte cell marker GFAP (human-specific GFAP antibody, **hGFAP**). Scale bars: A-G, 580 µm, H, 550 µm; I, 100 µm; J, 300 µm; K, 2.8 µm; L-M, 3 µm; N, 4 µm; O-P, 12 µm; Q, 30 µm; R, 5 µm; S, 90 µm; T, 8 µm.

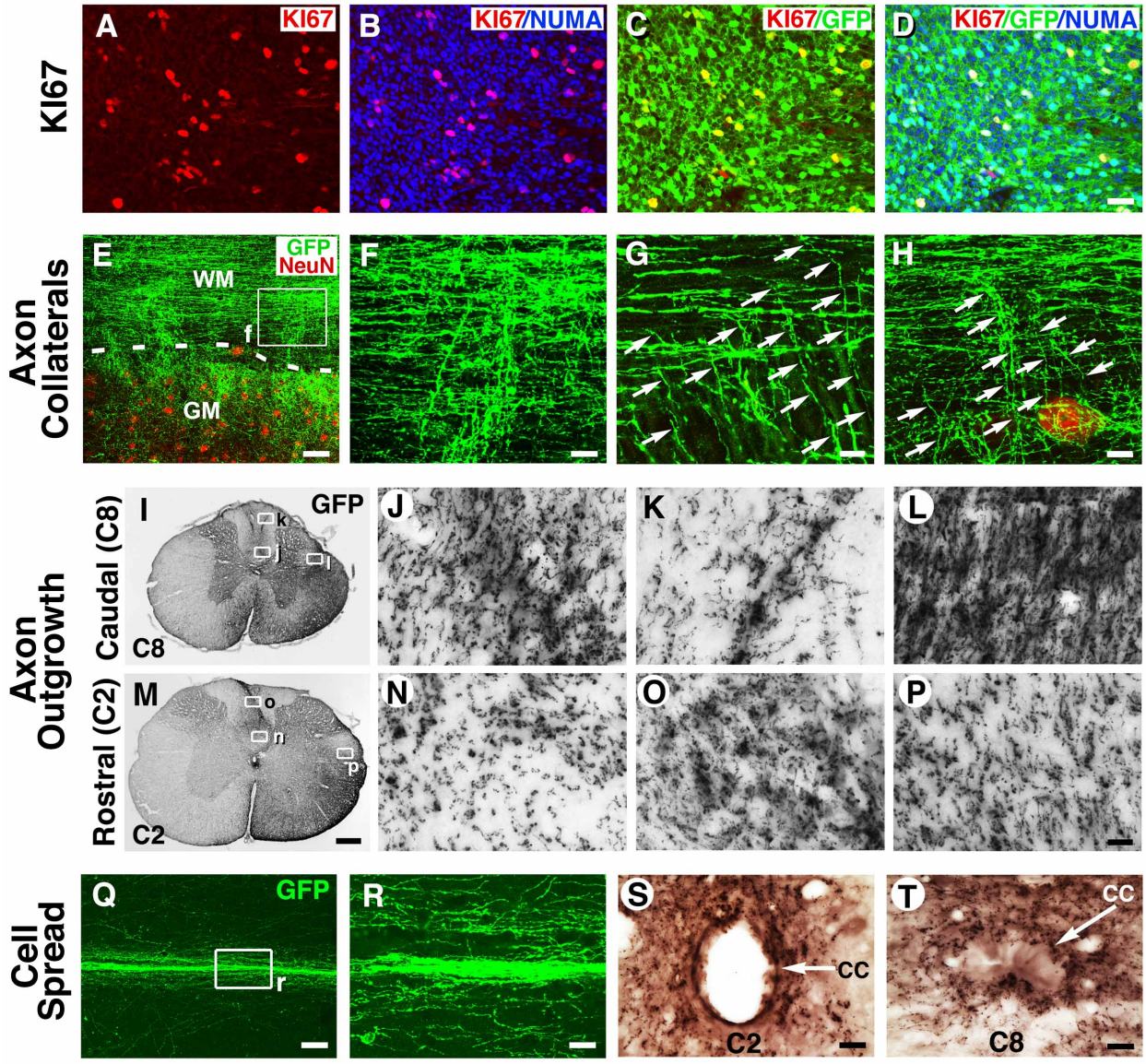

Suppl. Fig 3 (Related to Main Fig. 2): Ki67 Labeling in Graft, Collateral Growth of Human Axons, Caudal (C8) and Rostral (C2) Distribution of Human Axons, and Graft Spread into Central Canal

(A-D) Ki67, NUMA and GFP triple immunoflorescent labeling shows **(A)** Ki67 positive cells in human iPSC graft specifically labeled by **(B)** NUMA and **(C-D)** GFP, indicating proliferation of some grafted cells. (**E-H**) GFP and NeuN double labeling reveals that human axons in host white matter (**WM**) give off branches that penetrate host gray matter (**GM**). **F** is higher magnification view from boxed area in panel E. **(G-H)** Examples of multiple collaterals (arrows) branching off from human axons in host white matter toward host gray matter. (**I**) Distribution of **GFP** labeled human axons at C8, three segments caudal to the iPSC graft in the C5 lesion site. **(J-L)** Higher magnification views from boxed area in I show distribution of human axons in **(J)** ventral dorsal column, **(K)** the cuneate and gracile funiculi, and **(L)** dorsolateral funiculus. (**M-P**) Distribution of **GFP** labeled human axons at C2, three segments rostral to the iPSC graft in the C5 hemisection. **(M)** Low and **(N-P)** higher magnification views. **(Q)** GFP-labeled iPSCs are present in the central canal region of the spinal cord, as seen in a

horizontal section located one spinal segment rostral to the C5 lesion site. (**R**) Higher magnification of boxed region in **Q** shows GFP-expressing cells in central canal, with nearby GFP-expressing axons in host spinal cord. (**S**) Graft cell accumulation in the central canal is not observed in animals more than three spinal segments from the C5 lesion site; shown is a patent central canal (**CC**) at the C2 level lacking GFP-labeled cells. GFP is light level, brown reaction product. Transverse section. (**T**) Similarly, cells were not observed in the central canal at spinal segments caudal to the lesion site. Shown is the C8 spinal segment in transverse orientation. Note that the central canal is closed at this level, a frequent occurrence in adult rats. GFP-labeled axons are present in surrounding host tissue, derived from graft in the lesion site located three segments rostrally. Scale bar: A-D, 32 μm; E, 64 μm; F, 16 μm, G, 12 μm; H, 14 μm; I, M, 300 μm; J-L, N-P, 30 μm; Q, 90 μm; R, 22 μm; S-T, 23 μm.

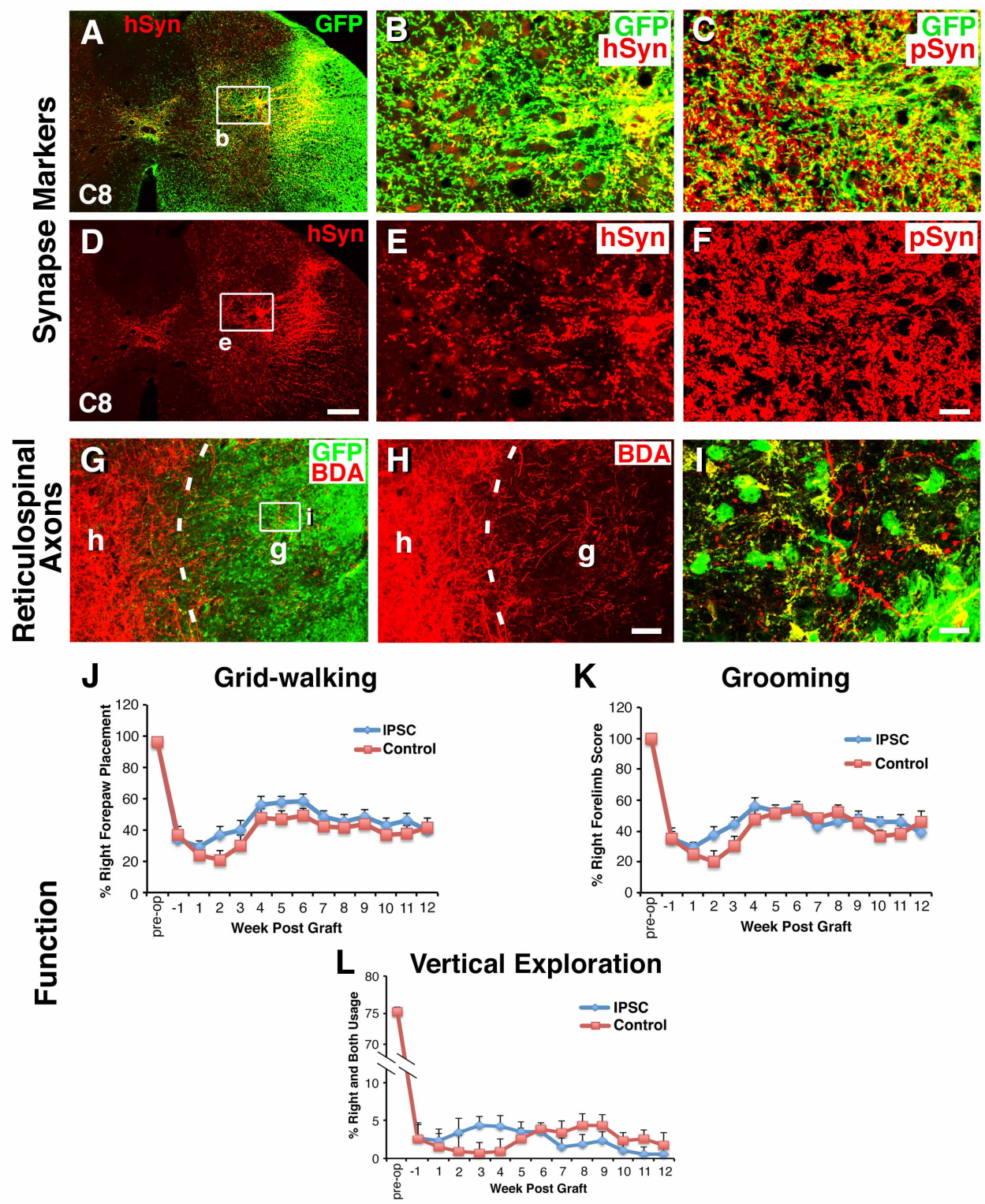

Suppl. Fig. 4 (Related to Main Fig. 3-4): Human-Specific Synaptophysin Expression, Host Reticulospinal Axonal Growth, and Functional Outcomes
(**A, D**) **GFP** and human-specific synaptophysin (**hSyn**) labeling at C8, three spinal segments caudal to the lesion site. **B, E** are higher magnification views from boxed area in panels **A, D**. (**C, F**) Pan-synaptophysin (**pSyn**) label detects rodent and human synaptophysin. (**G**) Host reticluospinal axons anterogradely labeled with **BDA** penetrate (**G**) **GFP**-expressing iPSC-NSC grafts in the lesion site (**G** and **H** are the same section).

(**I**) Higher magnification view from boxed area in panel G demonstrates reticluospinal axons within the iPSC graft. Scale bar: A, D, 128 µm; B, E, C, F, 24 µm; G-H, 100 µm; I, 2.5 µm. **(J-L)** Behavioral outcomes were measured weekly on three tasks after C5 hemisection: **(J)** grid-walking, **(K)** grooming, and **(L)** vertical exploration. N= 7, **iPSC** grafted group; N=5, **Control** group. No significant behavioral improvement was observed (Manova repeated measures).

SUPPLEMENTAL EXPERIMENTL PROCEDURES

Generation and Differentiation of Human iPS cells and NSCs

Methods for generating human induced pluripotent stem cells (iPSCs) and driving them toward a neural stem cell lineage have been published previously (Yuan et al., 2011; Israel et al., 2012). Briefly, primary fibroblasts were cultured from dermal punch biopsies of an 86 year-old normal control human male. Fibroblasts were transduced with retroviral vectors expressing OCT4, SOX2, KLF4, and c-MYC. The generated IPS cell line (NDC1, Israel et al., 2012) was cultured on PA6 cells for induction of neural stem cells in the presence of SMAD inhibitors, Noggin (500 ng/mL) and SB431542 (10 μM), and was FACS-purified using $CD184^{+}$, $CD15^{+}$, $CD44^{-}$, and $CD271^{-}$ (Yuan et al., 2011). Purified neural stem cells were then cultured on poly-ornithine/laminin-coated plates with DMEM/F12 supplemented with N2, B27 and basic fibroblast growth factor. Proliferating neural stem cells were then transduced with lentiviral vectors expressing green fluorescent protein (GFP) under CAG promoter (Taylor et al., 2006) to allow in vivo tracking and assessment of process extension.

In Vivo Studies:

A total of 14 adult female athymic nude rats (T-cell deficient; Harlan Laboratories) weighing 180-200 grams were subjects of this study. 7 rats received human iPSC-derived NSC grafts, and 5 were controls; all these rats underwent weekly behavioral analysis and survived for 3 months post-grafting. Two additional subjects were grafted and dedicated to ultrastructural analysis (see below). NIH guidelines for laboratory animal care and safety were strictly followed. Animals were deeply anesthetized using a combination (2 ml/kg) of ketamine (25 mg/ml), xylazine (1.3 mg/ml) and acepromazine (0.25 mg/ml) under aseptic conditions. C5 lateral hemisection lesions were placed as previously described (Lu et al., 2012a) to assess survival, integration and axonal extension from grafted human iPSC-derived NSCs. Briefly, following C5 dorsal laminectomy, the dura was cut longitudinally and retracted. A 1.5-mm-long block of the right spinal cord was excised using a combination of iridectomy scissors and microaspiration, with visual verification to ensure complete transection ventrally, medially and laterally. The lesion was closed. Two weeks later, cultured human iPSC-derived NSCs were trypsinized, washed with PBS and re-suspended at a concentration of 250,000 cells/μl. Cells were mixed into a fibrin matrix containing a growth factor

cocktail to promote survival and retention in the lesion site, as previously described (Lu et al., 2012b); without the fibrin matrix and growth factor cocktail, cells dispersed from the lesion site resulting in incomplete filling of the lesion. 5μl of the human iPSC-derived NSC mixture in fibrin and growth factor cocktail, or the fibrin and growth cocktail alone (lacking NSCs, in controls), were micro-injected into the sub-acute lesion cavity using a pulled glass micropipette with an inner diameter of 40 μm, connected to a PicoSpritzer II (General Valve, Fairfield, NJ). Cells were injected into 6 sites encompassing the lesioned hemicord: two side-by-side injections were made at the center of the lesion cavity, spaced 0.5mm apart (in the mediolateral plane); two side-by-side injections were made 0.5mm rostral to the center of the lesion site, spaced 0.5mm apart (in the mediolateral plane); and two side-by-side injections were made 0.5mm caudal to the center of the lesion site, spaced 0.5mm apart (in the mediolateral plane). Approximately 1μl per site of cell matrix was injected, for a total volume of approximately 5-6μl. Injections were stopped if reflux occurred. Animals were assessed weekly on grid walking, forelimb grooming and vertical exploration tasks for three months (Schallert et al., 2000; Gensel et al., 2006; Sandrow et al., 2008; Lu et al., 2012a). Baseline scores after C5 hemisection lesions were measured and treatment and control groups were matched for the extent of functional deficits prior to grafting. For the grid-walk task, footfalls were measured as animals walked on a 38cm^2 plastic-coated wire mesh field containing 3cm^2 openings, in five-minute test sessions recorded on video. Each forepaw was scored for the total number of steps and the total number of missteps. The total number of steps and missteps were added together to obtain the total number of placements. By convention, the right forepaw correct placement was calculated by dividing the number of steps by the total number of placements (steps plus missteps) (Gensel et al., 2006; Lu et al., 2012a). For forelimb grooming, cool tap water was applied to the animal's head and back with soft gauze, and grooming activity was recorded with a video camera. Subjects were scored for the regions of the head contacted by each forepaw during grooming, as reported previously (Gensel et al., 2006; Lu et al., 2012a). Performance was reported as score on the lesioned side (right) as percentage of score on the intact side (left). For the vertical exploration task, subjects were placed into a clear cylinder measuring 30 cm in height and 15 cm in diameter and their forelimbs were recorded by a video camera as they explored the cylinder wall

(Schallert et al., 2000). The number of times the subjects reached up and touched the wall with the left forelimb (intact), right forelimb (lesioned), or both simultaneously was counted. The frequency of injured forelimb usage was expressed by convention as the percentage of total ipsilateral (right) forelimb usage (lesioned right forelimb only plus both forelimbs simultaneously) divided by the total number of all forelimb usage (left forelimb only plus right forelimb only plus both forelimbs simultaneously). After behavioral testing, subjects underwent anterograde tracing of reticulospinal motor axons by injecting 2µl of a 10% biotin dextran amine (BDA, 10,000 MW, D1956, Invitrogen) solution into the right gigantocellular reticular nuclear (0.5µl /site); animals survived an additional two weeks (Lu et al., 2012a).

For cell fusion studies, human iPSC-derived NSCs were transduced with lentiviral vectors expressing red fluorescent protein (RFP) under the CAG promoter (Taylor et al., 2006). RFP-transduced NSCs (97% transduction efficiency) were then grafted into the C5 hemisection lesion site (one week after the lesion was placed) in adult SCID mice that transgenically express GFP (NOD.Cg-*Prkdcscid* Tg(CAG-EGFP)1Osb/KupwJ from The Jackson Laboratory; Niclou et al., 2008; N=4). Subjects survived for one month.

Anatomical Analysis: Spinal cords were sectioned on a cryostat set at 35µm intervals (Lu et al., 2012b) and processed for: 1) GFP labeling, to assess grafted cell survival, differentiation and processes outgrowth (GFP rabbit primary polyclonal, Invitrogen @ 1:1,500); 2) neural cell markers, including Tuj1 for immature and mature neurons (mouse monoclonal, Chemicon @ 1:500), NeuN for mature neuronal nuclei (mouse monoclonal, Chemicon @ 1:200), MAP-2 for mature neurons (mouse monoclonal, Chemicon @ 1:10,000 and rabbit polyclonal, Chemicon @ 1:250); choline acetyltransferase for mature spinal motor neurons (ChAT; goat polyclonal, Chemicon @ 1:200), neurofilament (NF; mouse from Chemicon @ 1:1500 to label axons), serotonin for mature raphespinal neurons and axons (5HT, rabbit polyclonal, ImmunoStar, @ 1:10,000), synaptophysin for pre-synaptic proteins expressed on both human and rodent synapses (Syn, mouse monoclonal, Chemicon @ 1:1000), human-specific synaptophysin for pre-synaptic proteins (hSyn, mouse monoclonal, Chemicon @ 1:1000), human-specific nuclear mitotic apparatus protein for grafted human cells (hNUMA, mouse monoclonal, Novocastra Lab at 1:200); glial fibrillary acidic protein for

astrocytes (GFAP, mouse monoclonal, Chemicon @ 1:1500); human-specific glial fibrillary acidic protein for astrocytes (hGFAP, mouse monoclonal, Millipore @ 1:1500); myelin basic protein to label myelin (MBP, 1:200, rabbit polyclonal, Millipore), Adenomatous Ployposis Coli to label oligodendrocytes (APC, mouse monoclonal, Oncogene @ 1:400), NG2 to label immature oligodendrocytes (rabbit polyclonal, Chemicon @ 1:200), collagen type IV (rabbit polyclonal, Biogenex @1:500), and Ki67 to label proliferating cells (rabbit polyclonal, Millipore @ 1:100). Sections were incubated overnight at 4^{o}C for primary antibodies, then incubated in Alexa 488, 594 or 647 conjugated goat or donkey secondary antibodies (1:250, Invitrogen) for 2.5 hr at room temperature.

Neural cell differentiation was determined by counting individual cells labeled for NeuN, GFAP, and ChAT within a fixed box size of 1024 x 1024 pixels at 1200X magnification within the graft, divided by the total number of cells per sample box labeled with human nuclear antigen NUMA. Two randomly selected fields from the graft epicenter were counted in each subject for each label. An average of 57 NeuN, 13 GFAP, and 3 ChAT labeled cells were counted in each of seven grafted animals, respectively, and divided by the mean number of hNUMA-labeled nuclei in the sampled field (no cells in grafts were labeled for APC/hNUMA). Similar methods were used to quantify Ki67-labeled cells divided by NUMA number to obtain percentage of Ki67 cells in the graft.

The number of GFP-labeled human axons emerging from a typical graft placed at the C5 hemisection site was quantified using StereoInvestigator (MicroBrightField, mbfbioscience.com), as previously described (Lu et al., 2012b). Briefly, in every 6th horizontal section, a mediolateral line was drawn 500μm caudal to the graft/host interface under 40X magnification. The tissue was then examined under 600X magnification, and GFP-labeled axons that intersected this line were marked and counted. The sampling fraction was 16.7%.

The density of human-specific synaptophysin punctae was quantified in the intermediate spinal gray matter (Rexed Laminae VI-VII) in cross sections at the C8 spinal level in each animal that received human iPSC grafts (n=7). The number of pixels occupied by human synaptophysin within a fixed box size of 1024 x 1024 pixels at 400X

magnification view was measured using Image J software, as previously described (Lu et al., 2005). Thresholding values were chosen such that only immunolabeled synaptophysin was measured, and light nonspecific background labeling was not detected. We then quantified the density of pan-synaptophysin-labeled punctae, which detects both rodent and human synaptophysin, in the same region using the same methods. The proportion of synaptic protein in this region derived from human axons was expressed as the amount of hSyn label divided by the amount of pan-Syn label in the same sampling frame.

The number of 5-HT labeled serotonergic axons penetrating grafts in lesion sites was quantified using StereoInvestigator, as previously described (Lu et al., 2012a). Briefly, a series of 1-in-12 sections were labeled for 5-HT to visualize serotonergic axons. The rostral lesion/graft border was defined as a region in which there was an upregulation of GFAP labeling, and a change in the regularity and consistency of cellular distribution, from uniform in host gray and white matter to irregular and containing dispersed neurons in grafted tissue. The number of axons crossing lines within the graft placed at 250, 500 and 1000μm distances from the rostral host/lesion border were counted at 400X magnification. Quantifiers were blinded to group identity.

Two additional subjects that underwent C5 lateral hemisections and iPSC grafts survived for three months and were used for electron microscopic analysis of synapse formation and myelination of human axons according to the methods of Knott et al. (2009). Briefly, subjects were perfused with 4% paraformaldehyde and 0.25% glutaraldehyde. Vibratome coronal sections 3 mm caudal from the graft/lesion site were sectioned on a cryostat set at 40μm intervals and processed for light-level observation of GFP immunolabeling using DAB and nickel chloride. Both the host spinal cord gray matter and lateral white matter containing GFP-labeled axons were then microscopically dissected and post-fixed with 1% osmium tetroxide, dehydrated, embedded in Durcupan resin. These samples were sectioned at 60 nm thickness using an ultramicrotome. Individual BDA-labeled axons or axonal terminals were located and assessed using an FEI 200KV Sphera microscope at the UCSD CryoElectron Microscopy Core Facility.

Statistical Analysis. In all quantification procedures, observers were blinded to the nature of the experimental manipulation. Two-group comparisons were tested by Student's t-test (JMP software) at a designated significance level of $P<0.05$. Data are presented as mean ± SEM. For behavioral analysis, repeated measures ANOVA was used to assess group differences over time.

Supplemental References

Gensel, J.C., Tovar, C.A., Hamers, F.P., Deibert, R.J., Beattie, M.S., and Bresnahan, J.C. (2006). Behavioral and histological characterization of unilateral cervical spinal cord contusion injury in rats. J. Neurotrauma 23, 36-54.

Knott, G.W., Holtmaat, A., Trachtenberg, J.T., Svoboda, K., and Welker, E. (2009). A protocol for preparing GFP-labeled neurons previously imaged in vivo and in slice preparations for light and electron microscopic analysis. Nat. Protoc. 4, 1145-1156.

Lu, P., L. Jones, M. Tuszynski. (2005). BDNF-expressing marrow stromal cells support extensive axonal growth at sites of spinal cord injury. Exp Neurol. 191, 344-360.

Sandrow, H.R., Shumsky, J.S., Amin, A., and Houle, J.D. (2008). Aspiration of a cervical spinal contusion injury in preparation for delayed peripheral nerve grafting does not impair forelimb behavior or axon regeneration. Exp. Neurol. 210, 489-500.

Schallert, T., Fleming, S.M., Leasure, J.L., Tillerson, J.L., and Bland, S.T. (2000). CNS plasticity and assessment of forelimb sensorimotor outcome in unilateral rat models of stroke, cortical ablation, parkinsonism and spinal cord injury. Neuropharm 39, 777-787.